Electronic Supplementary Material (ESI) for Nanoscale.

Supplementary Notes on "First principle investigation of Tunnel FET based on nanoribbons from topological two-dimensional material"

E. G. Marin,* D. Marian,* G. Iannaccone, and G. Fiori†

Dipartimento di Ingegneria dell'Informazione,

Università di Pisa, Pisa, 56122, Italy.

* These authors contributed equally to this work.

† email: gfiori@mercurio.iet.unipi.it

Supplementary Note 1.

As discussed in S[1, 2], silicene and germanene nanoribbons show very distinct topological properties depending on whether they are armchair or zig-zag. In particular, contrary to armchair nanoribbons, zig-zag nanoribbons present localized edge states. To check that the stanene is not an exception in the group IVa family, we have considered armchair and zig-zag stanene nanoribbons with $\sim$ 4 nm width, corresponding to 17 and 12 stanene lines in the armchair and zig-zag configurations.

Armchair nanoribbons have a non-magnetic ground state. For zig-zag nanoribbons, the ground state is theoretically antiferromagnetic S[3], but the inter-edges interaction is expected to be strongly weakened by thermal fluctuations for $\sim$ 4 nm width S[4, 5], and non-magnetic ground states are more likely to be observed at room temperature. For this reason, we have considered here non-magenetic ordering also for zig-zag nanoribbons.

Density Functional Theory computations have been performed through the Quantum Espresso v 5.2.0 package S[6]. Spin orbit interaction (SOI) has been taken into account by means of a non-collinear spin polarized calculation. The details of the DFT calculations are specified in the Methods. Fig. S1 shows a top view of the geometric structure (left panel) of the a) armchair and b) zig-zag stanene nanoribbons. The unit cells are boxed in black rectangles. The presence of localized states in both configurations have been checked by calculating the normalized contribution of the edge atoms to the density of states (DOS) projected on the bands, computed on a highly symmetric path in the 1D Brillouin zone (central panel). The contribution of the center atoms has also been computed (right panel). Edge and central atoms are identified in the left panel by red and blue circles, respectively.

For armchair nanoribbons, the bandstructure shows a linear dispersion relation close to the Fermi level (used as energy reference). These semi-metallic states are, however, not topological localized states as can be clearly appreciated from the normalized contribution of the edge atoms to the bands in this region. This is not a matter of the definition of the edge atoms. We have tested DOS projections on the bands considering more atoms close to the edges without qualitative changes. The mixing of edge and central atoms contributions to the states is not even a consequence of a insufficient width of the nanoribbon. We have checked that the mixing is present for wider armchair nanoribbons where semi-metal states are present. The semi-metallic states in armchair nanoribbons appears with a periodicity

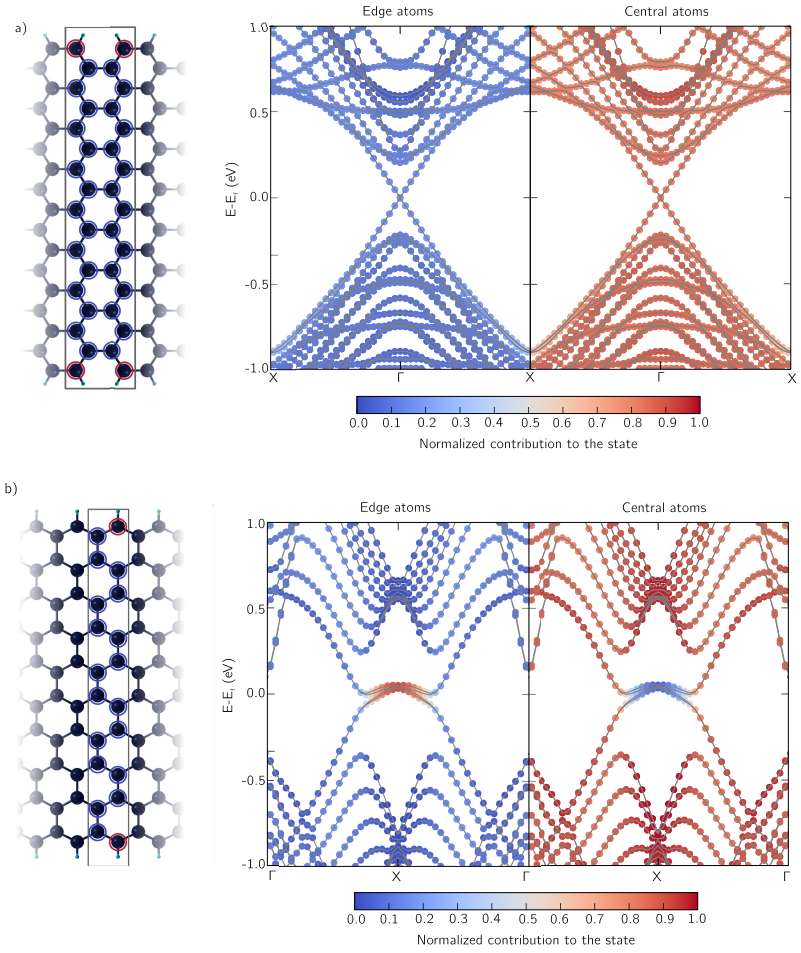

FIG. S1. **Density of states projected on the bandstructure of non-magnetic armchair and zig-zag stanene nanoribbons.** Top view of the geometric structure of a) armchair and b) zig-zag stanene nanoribbons with $\sim$ 4 nm width. This corresponds to 17 and 12 stanene lines in the armchair and zig-zag nanoribbons, respectively. The elementary cell is boxed by a black rectangle. The edge atoms are marked with red circles, and the central atoms are marked with blue circles. Normalized contribution of the edge (center panel) and central (right panel) atoms to the DOS projected on the bands for the a) armchair b) zig-zag stanene nanoribbons. The Fermi level is set to 0 eV.

of 3 armchair lines S[3, 7]. The result is coherent with the conclusions on germanene and silicene presented in the literature S[1, 8, 9].

In the zig-zag nanoribbon instead, edge atoms fully contribute to the states close to the Fermi level, and central atoms contribute elsewhere. Similarly to germane and silicene, these edge localized states show a strong non-linear dispersion relationship, which cannot

be explain by simple 1-orbital tight-binding models as demonstrated in S[1].

Supplementary Note 2.

The multiscale approach requires the translation of the Bloch-waves basis, obtained through Quantum Espresso DFT S[6], into a tight-binding-like basis set. The computational burden of a self-consistent device simulation is, otherwise, unaffordable. The localization procedure was accomplished employing Wannier90 code S[10], computing Maximally Localized Wannier Functions and providing an equivalent, but lighter description of the DFT results. For electronic transport calculations, only the bands close to the Fermi level are relevant. The Wannierisation process was therefore performed for the 8 bands (spin degeneracy not included) closer to the Fermi level, 4 conduction bands and 4 valence bands. Initial projections on p_z orbitals of Sn was considered. 16 MLWF resulted from the process. A comparison of the DFT and Wannier bandstructure in a highly symmetric path along the 1D Brillouin zone is shown in Fig. S2. DFT results are depicted as blue empty diamonds, while red solid lines are used for MLWF.

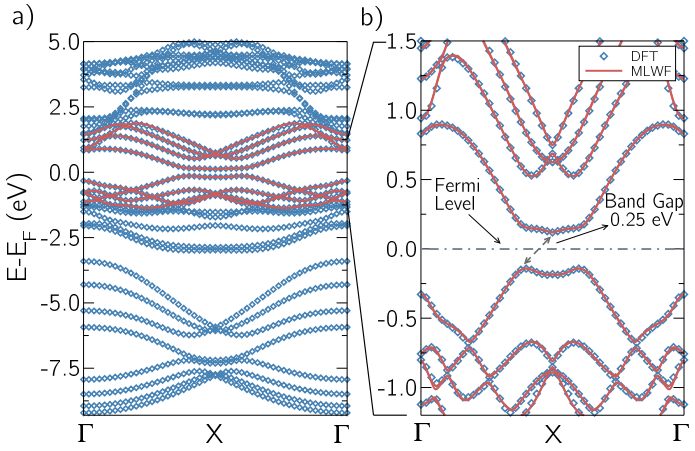

FIG. S2. **Wannierisation of the DFT electronic bandstructure.** Energy bands along a high symmetry path in the 1D Brillouin zone. Density Functional Theory calculations are denoted by empty blue diamonds, while red solid lines stand for MLWF computations. The Fermi level is set as zero reference for energies and is plotted as a dash-dotted gray line.

Supplementary Note 3.

To clarify if the localized states in the stanene ZZ-NR with antiferromagnetic ordering are topologically protected, we have computed the expectation value of the bandstructure states of the $\hat{S}_z$ spin operator. All DFT calculations has been performed within the Quantum Espresso package v 5.2.0 S[6]. The results are shown in Fig. S3 for a) positive and b) negative expectation values of $\hat{S}_z$.

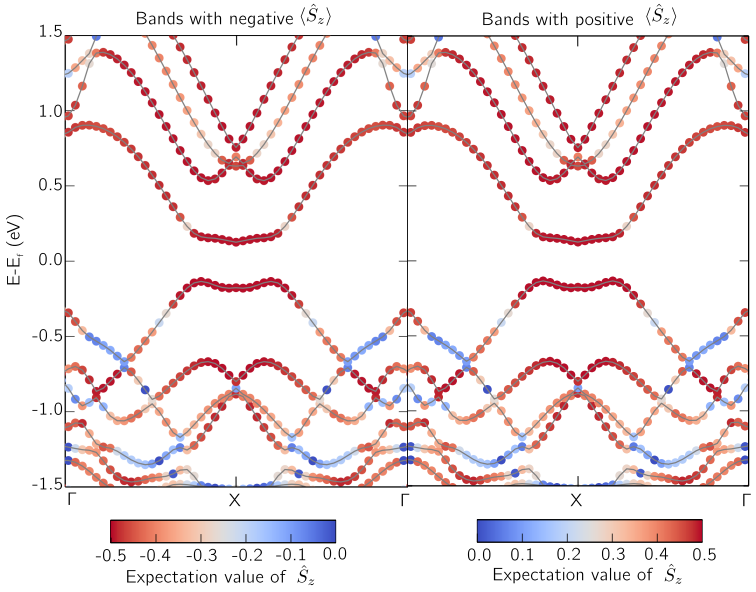

FIG. S3. **Spin projection on the electronic bandstructure of the stanene nanoribbon.** Bands with a) a negative and b) a positive expectation value of $\hat{S}_z$. The color determines the expectation value in each case.

The bands associated to the localized states around the CBM and VBM (see Fig. 3) show $\langle \hat{S}_z \rangle$ of $\sim +1/2$ or $\sim -1/2$, coherently with the strong and opposite magnetization at the edges observed in Fig. 2. It has been confirmed by additional projections of the density of states that both edges contribute to the CBM and VBM in equal proportion. The presence of bands with similar energy for positive and negative values of $\hat{S}_z$ refutes any chance of having topologically protected states in the antiferromagnetic configuration. Transitions from a $+k$ to a $-k$ state (the 1D Brillouin zone shows symmetry around the Γ-point) in the CB or the VB are possible within the same spin component and therefore the states are not protected S[11].

Supplementary Note 4.

The DOS integrated along a highly symmetric path in the Brillouin zone, further confirms previous considerations. As can be observed, edge atoms mostly contributes to the CB and VB edges, while central atoms elsewhere.

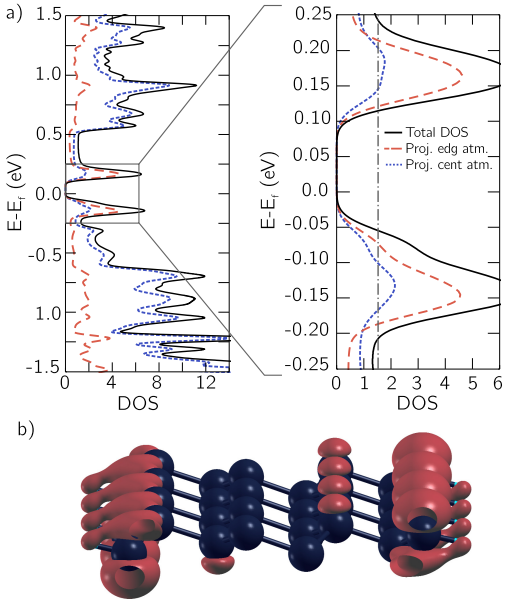

FIG. S4. **Total density of states.** a) Integrated density of states (DOS) (black curve) and projections of the DOS on the edge (red dashed curve) and central atoms (dotted blue curve). The Fermi level is set to zero. Right panel: zoom around the Fermi level. b) Spatial distribution of the DOS for a value 1.5 states/eV in the range of energies $|E - E_f| < 0.25$eV. The dominant role of the edges in the vicinity of the Fermi level is consistent with the spatial distribution of high values of the DOS. The unit cell has been replicated 4 times along the nanoribbon length for visualization purposes.

Supplementary Note 5.

As explained in the Supplementary Note 3, the localized states are not protected against back-scattering. The transport along the 1D-channels at the edges of the TFET can, therefore, be strongly degraded by line edge roughness resulting from uncontrolled processes during the fabrication. The sensitivity of the TFET transfer characteristic to different percentages of defects was discussed in the main text by forcing the on-site energies of the tight-binding Hamiltonian (see Methods for more details). An alternative, but equivalent, study has been performed from DFT computations.

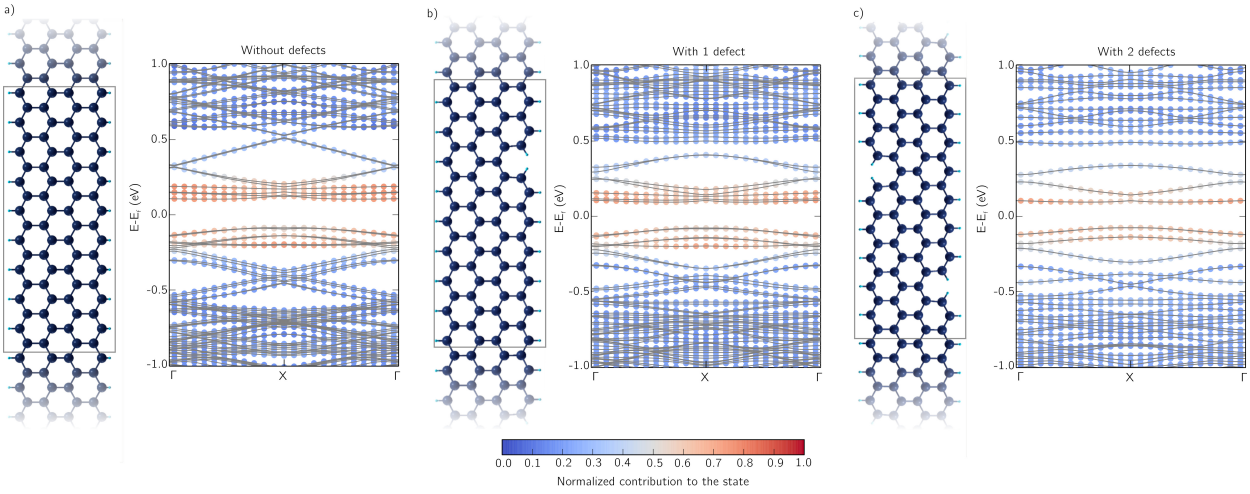

FIG. S5. **Density of states projected on the electronic bandstructure for different number of defects.** Normalized contribution of the edge atoms to the bands projected-DOS for a) ZZ stanene nanoribbon without defects. b) ZZ stanene nanoribbon with 1 vacancy on the left edge every 9 atoms. c) ZZ stanene nanoribbon with 2 vacancies, 1 on each edge, every 9 edges atoms. The normalized holds the idea that the localized states keep present in spite of the removal of some edge atoms. The *super*-unit cell of the nanoribbon is boxed in a grey rectangle.

As in the main text, a zig-zag stanene nanoribbon with antiferromagnetic ordering was studied, but a *super*-unit cell composed of 9 elementary unit cells was built. The *super*-unit cell allows us to force some defects at the borders without removing them completely (in the elementary unit cell each edge comprised only 1 atom, see Fig. 1) and check if localized states are still present. DFT computations were performed by means of Quantum Espresso S[6]. A structural optimization of all geometries was performed within the Broyden-Fletcher-Goldfarb-Shanno algorithm until forces were less than 5×10^{-3}eV/Å. The details

of the DFT calculations do not differ from the main text. Fig. S5 shows the normalized contribution of the edge atoms to the density of states (DOS) projected on the bands on a highly symmetric path along the 1D Brillouin zone for a ZZ-NR *super*-unit cell: without defects (right), with 1 defect at one border (center), and with 1 defect at each border (left). Although some bands are lost when defects are introduced, localized states around the Fermi level (used as reference here) are present. The *super*-unit cell is boxed in a grey rectangle in every case. The persistence of the localized bands and the spatial distribution of high values of the DOS at the edges, reinforce the conclusion about the robustness of the 1D channels to LER.

Supplementary Note 6.

To simulate line edge roughness we force the on-site energies of the MLWF in which a defect was introduced to a large value, thus emulating the presence of a barrier. An additional and more robust check consist of setting to zero in the Hamiltonian also the coupling terms to this site, avoiding this way the possibility of hopping. Figure S6 shows the comparison between both methods. Both methodologies lead to equivalent results but the latter is less stable in terms of convergence of the self-consistent loop between Poisson and NEGF.

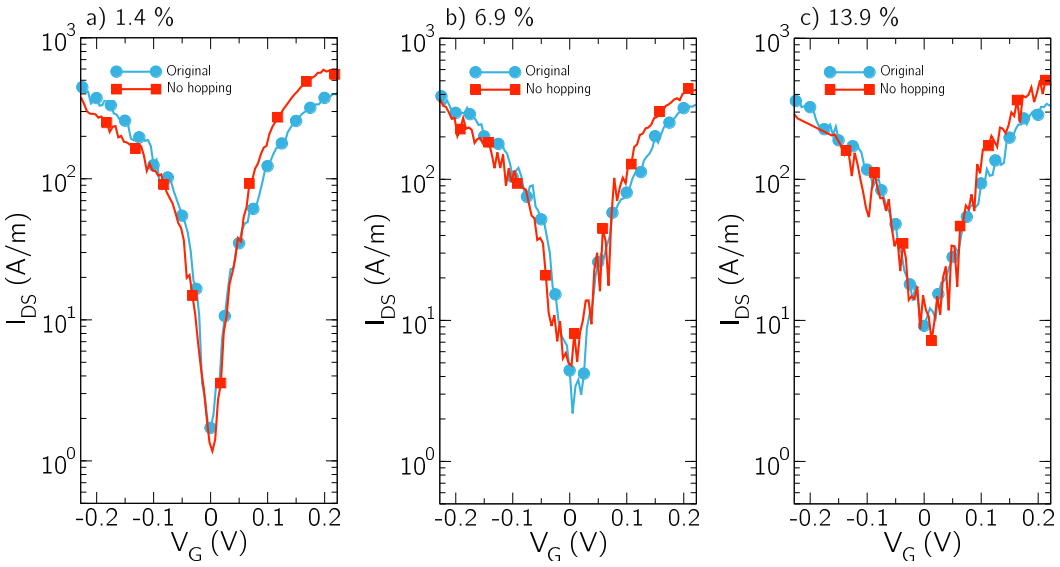

FIG. S6. **Transfer characteristics of the TFET for different percentages of defects at the edges.** a) 1.4%, b) 6.9% and c) 13.9%, as without (blue circles) and when setting (red squares) the coupling terms to in the Hamiltonian to zero.

S[1] Mathes, L., and Bechstedt, F. Influence of edge and field effects on topological states of germanene nanoribbons from self-consistent calculations, *Phys. Rev. B*, **90,** 165431. 2014.

S[2] Le, N. B., Huan, T. D., Woods, L. M. Tunable Spin-dependent properties of zig-zag silicene nanoribbons *Phys. Rev. Appl.*, **1,** 054002. 2014.

S[3] Xiong, W., Xia, C., Peng, Y., Du, J., Wang, T., Zhang, J., et al. Spin-orbit coupling effects on electronic structures in stanene nanoribbons. *Phys. Chem. Chem. Phys.*, **18,** 6534. 2016.

S[4] Jung, J., Pereg-Barnea, T., and MacDonald, A.H. Theory of interedge superexchange in zig-zag edge magnetism. *Phys. Rev. Lett.*, **102,**, 227205. 2009.

S[5] Yazyev, O. V. Emergence of magnetism in graphene materials and nanostructures. *Rep. Prog. Phys.*, **73,** 056501. 2010.

S[6] Giannozzi, P., Baroni, S., Bonini, N., Calandra, M., Car, R., Cavazzoni, C., et al. QUANTUM ESPRESSO: a modular and open-source software project for quantum simulation of materials. *J. Phys.: Cond. Matt.*, **21,** 395502. 2009.

S[7] Houssa, M., van de Broek, B., Iordanidou, K., Lu, A. K. A., Pourtois, G., Locquet, J. P., et al. Topological to trivial insulating phase transition in stanene. *Nano Research*, **9,** 774. 2016.

S[8] Ezawa, M., and Nagaosa, N. Interference of topologically protected edge states in silicene nanoribbons. *Phys. Rev. B*, **88,** 121401. 2013.

S[9] Cahangirov, S., Topsakal, M., and Ciraci1, S. Armchair nanoribbons of silicon and germanium honeycomb structures. *Phys. Rev. B*, **81,** 195120. 2012.

S[10] Marzari, N., Mostofi, A. A., Yates, J. R., Souza, I., Vanderbilt, D. Maximally localized Wannier functions: theory and applications. *Rev. Mod. Phys.*, **84,** 1419. 2012.

S[11] Manoharan, H. C. Topological insulators: a romance with many dimensions. *Nat. Nanotech.*, **5,** 477. 2010.